

Effects of fines content on void ratio, compressibility, and static liquefaction of silty sand

Poul V. Lade[†]

Department of Civil Engineering, The Catholic University of America, Washington, D.C. 20064, U.S.A.

Jerry A. Yamamuro

School of Civil and Construction Engineering, Oregon State University, Corvallis, Oregon 97331, U.S.A.

Carl D. Liggio, Jr.

Pharos Enterprise Intelligence, LLC, 150 East 56th Street, Suite PHB, New York, NY 10022, U.S.A.

(Received February 12, 2009, Accepted March 5, 2009)

Abstract. Many aspects of the behavior of sands are affected by the content of non-plastic fine particles and these various aspects should be included in a constitutive model for the soil behavior. The fines content affects maximum and minimum void ratios, compressibility, shear strength, and static liquefaction under undrained conditions. Twenty-eight undrained triaxial compression tests were performed on mixtures of sand and fine particles with fines contents of 0, 10, 20, 30, 50, 75, and 100% to study the effects of fines on void ratio, compressibility, and the occurrence of static liquefaction. The experiments were performed at low consolidation pressures at which liquefaction may occur in near-surface, natural deposits. The presence of fines creates a particle structure in the soil that is highly compressible, enhancing the potential for liquefaction, and the fines also alter the basic stress-strain and volume change behavior, which should be modeled to predict the occurrence of static liquefaction in the field. The void ratio at which liquefaction occurs for each sand/fines mixture was determined, and the variation of compressibility with void ratio was determined for each mixture. This allowed a relation to be determined between fines content, void ratio, compressibility, and the occurrence of static liquefaction. Such relations may vary from sand to sand, but the present results are believed to indicate the trend in such relations.

Keywords: compressibility; fines; instability; silty sand; static liquefaction; triaxial tests.

1. Introduction

The occurrence of such disastrous events as failures of tailings dams (releasing large quantities of hazardous materials), flow slides occurring in gently inclined submarine slopes (tearing marine structures and communications cables apart), debris flows (fluidizing hillsides resulting in mud flows), and snow avalanches (trapping and burying skiers) have always been difficult to forecast,

[†] Professor, Corresponding author, E-mail: Lade@cua.edu

and they have presented a bit of a mystery, because these events do not appear to conform with conventional methods of analyses for slope failures as known to geotechnical engineers. They appear to be initiated by a form of instability that may occur in fine particulate materials such as loose, fine sands and silts, and in snow.

The underlying mechanism for these instabilities was discovered in the process of experimental studies of some theoretical aspects essential to the development of models for soil behavior (Lade *et al.* 1987, 1988). Research has subsequently been pursued to clarify the type of behavior and the conditions leading to instability and subsequent static liquefaction of these materials (Lade and Pradel 1990, Lade 1992, 1993, 1994a, 1994b). Several types of fine sands have been studied in different laboratory tests to find out which sand compositions are most susceptible to instability and static liquefaction (Yamamuro and Lade 1997, 1999, Lade and Yamamuro 1997, Zlatovic and Ishihara 1997).

It is the fact that loading of compressible, particulate material resulting in large plastic deformations can occur under decreasing stresses that leads to unstable behavior of water saturated granular materials under undrained conditions. This happens for conditions where the water cannot escape fast enough to avoid build-up of pore water pressures. Loose, fine sands have sufficiently low hydraulic conductivities that small amounts of volumetric creep may temporarily produce undrained conditions in such soils, and instability of the soil mass follows. The soil will continue to be stable as long as it remains drained, i.e. as long as the water can escape fast enough that pressures do not build up in the water.

Many factors such as compressibility, hydraulic conductivity, and creep play important roles in the stability of particulate materials. Here is presented an experimental study of the effects of the content of fine particles in a sand on (a) the range of void ratios, (b) the compressibility, and (c) the potential for static liquefaction.

2. 'Reverse' behavior at low confining pressures

Within a range of low confining pressures, drained tests on very loose, silty sand with high compressibility show negligible effect of magnitude of confining pressure on the contractive volume change, as shown in Fig. 1 (Yamamuro and Lade 1997). The corresponding undrained tests in the same range of confining pressures show development of essentially equal pore pressures, as indicated in Fig. 2, and consequently the effective confining pressures reach zero faster with decreasing initial consolidation pressures, as shown in Fig. 3. Thus, the lower the initial consolidation pressure the faster liquefaction conditions are reached in the specimens. This clearly shows that static liquefaction is a low-pressure phenomenon. The effect of increasing the confining pressure is to increase the resistance to liquefaction. This behavior is contrary to observed behavior for conventional undrained tests on clean sands.

This 'reverse' behavior observed for very loose, silty sand at low confining pressures is accompanied by an inflection in the instability line, as seen (exaggerated) in the schematic diagram in Fig. 4 (Lade and Yamamuro 1997). Four distinctly different types of effective stress paths with corresponding behavior patterns are shown. Static liquefaction occurs at the lowest pressures, and it is characterized by large pore pressure developments that result in zero effective confining pressure and zero stress difference at small axial strains. In this range, the maximum effective friction angle increases with increasing effective confining pressure and it continues to increase through the following region of

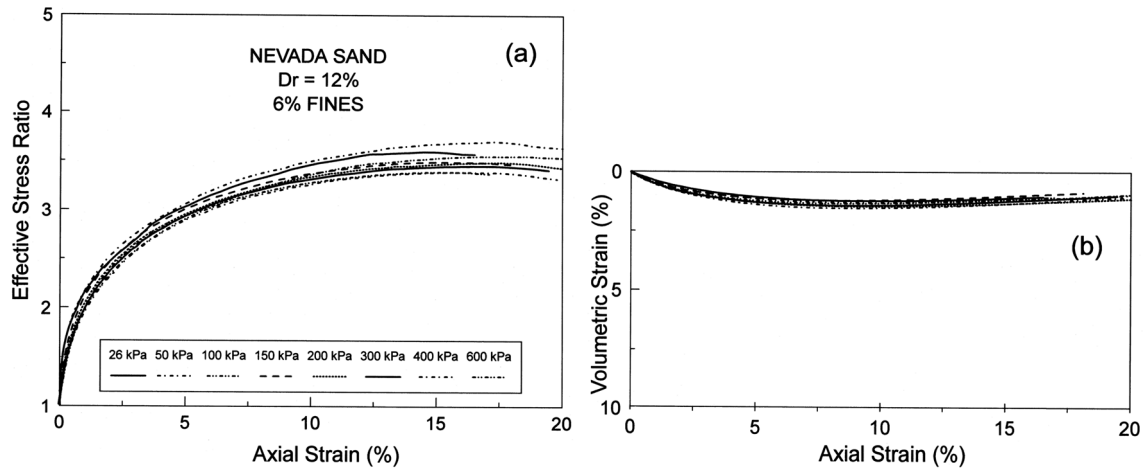


Fig. 1. Results of drained tests on Nevada sand at a relative density = 12% and with confining pressures from 26 to 600 kPa. (a) Effective stress ratio vs. axial strain curves, and (b) volumetric strain vs. axial strain curves that indicate large contractive volume change behavior and little effect of confining pressure (after Yamamuro and Lade 1997).

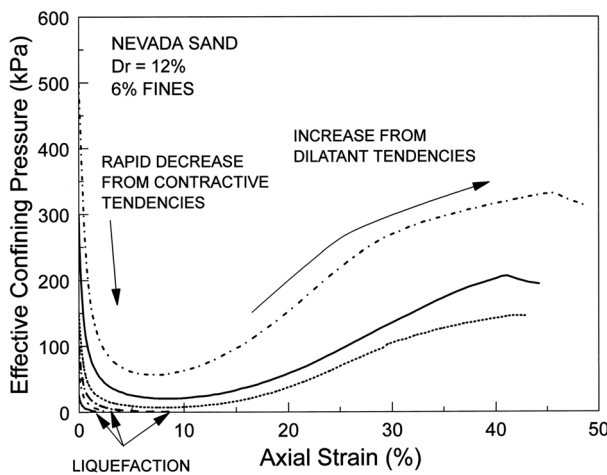


Fig. 2. Effective confining pressures during shearing from tests on Nevada sand at a relative density = 12%, showing that larger initial confining pressures have higher capacities to absorb rising pore pressures resulting in increased resistance to static liquefaction (after Yamamuro and Lade 1997).

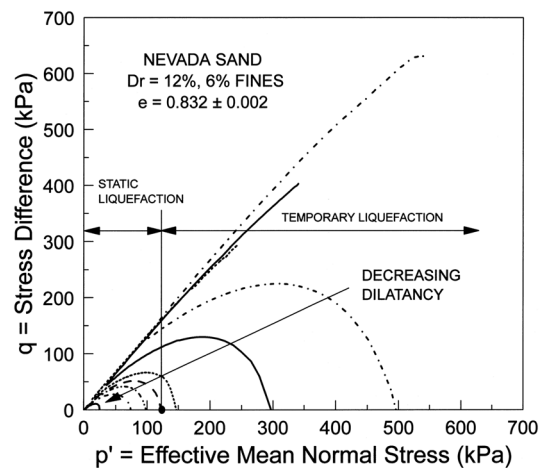


Fig. 3. Undrained effective stress paths shown in p'-q diagram for tests on Nevada sand at a relative density = 12% indicate complete static liquefaction below an initial confining pressure of 125 kPa and increasing resistance to liquefaction above that pressure (after Yamamuro and Lade 1997).

temporary liquefaction. This second region is characterized by an initial peak stress difference, followed by a decline. As shearing continues the stress path crosses the phase transformation line into the region of dilation and pore pressure decline, resulting in stress differences increasing to much higher magnitudes than the initial peak. In this region the specimens show increasing dilatancy with increasing initial consolidation pressure, contrary to conventional sand behavior. The following two regions of temporary instability and instability are those recognized from conventional sand

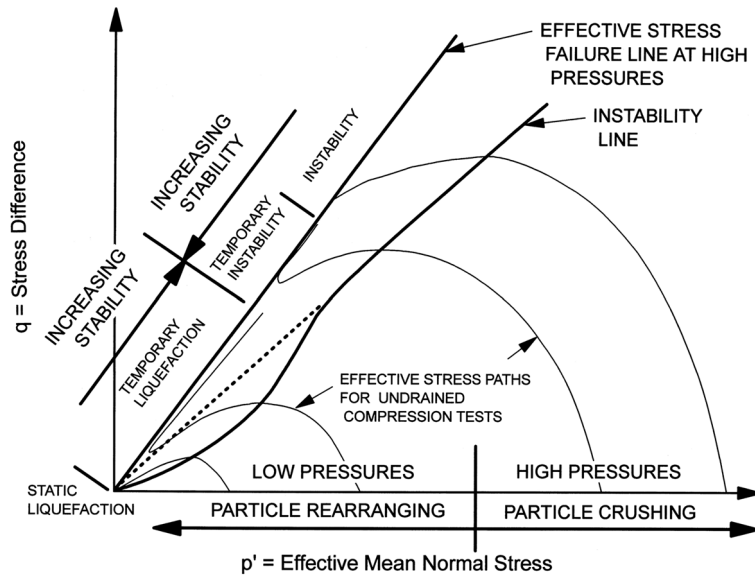


Fig. 4. Four distinctly different general types of undrained effective stress paths for loose silty sands: Static liquefaction, temporary liquefaction, temporary instability, and instability shown in p' - q diagram (after Lade and Yamamuro 1997).

behavior (Lade 1992, 1993, 1994a, 1994b).

This pattern of sand behavior is entirely controlled by the very high compressibility of the very loose, silty sand. The compressibility is in turn controlled by the amount of fines present in the sand. Experiments performed on Nevada sand (Yamamuro and Lade 1998) showed a correlation between the fines content, void ratio, volume compressibility and static liquefaction. To throw additional light on this behavior, a series of experiments was performed on a different, fine sand with variation of the silt content.

3. Experimental program

For the silty sand described below, the variations of maximum and minimum void ratios with fines content were first determined. This was followed by experiments to determine the compressibility of the silty sand for different fines contents and different relative densities. Finally, twenty-eight undrained triaxial compression tests were performed on mixtures of sand and silt to study the effect of fines content on the occurrence of static liquefaction. These undrained triaxial experiments were performed at a constant, low consolidation pressure of 25 kPa at which liquefaction may occur in near-surface, natural deposits due to so-called 'reverse' behavior, as explained above.

4. Sand and silt used

Ottawa sand with rounded particles was graded between the #50 U.S. sieve (with 0.300 mm openings) and the #200 U.S. sieve (with 0.074 mm openings). This basic fine sand was mixed with

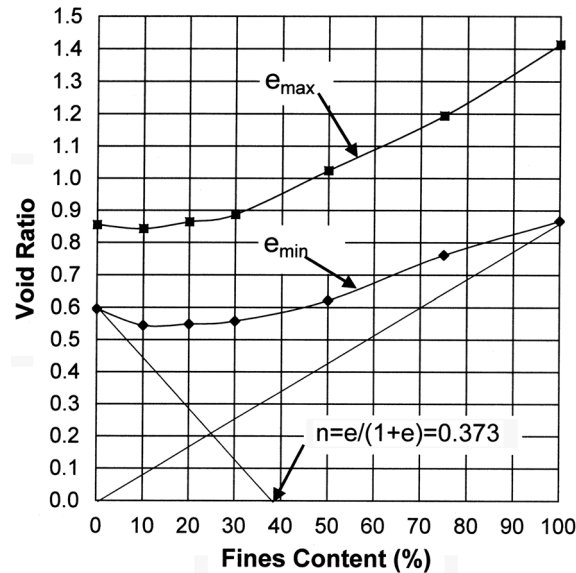


Fig. 5. Effects of fines content on maximum and minimum void ratios for silty sand consisting of fine Ottawa sand and Loch Raven fines.

Loch Raven silt consisting of particles in the silt range that passed the #200 U.S. sieve. The Ottawa sand had a specific gravity of $G_s = 2.65$ and the maximum and minimum void ratios were determined to be $e_{max} = 0.855$ and $e_{min} = 0.595$. The non-plastic Loch Raven silt was composed of angular quartz particles, and the portion passing the #200 U.S. sieve had a specific gravity of $G_s = 2.675$ and maximum and minimum void ratios of $e_{max} = 1.413$ and $e_{min} = 0.867$.

The fine Ottawa sand was mixed with Loch Raven silt to create mixtures with fines contents of 0, 10, 20, 30, 50, 75, and 100%. These mixtures were tested as described below.

5. Maximum and minimum void ratios

The variations of maximum and minimum void ratios with fines content were determined according to procedures described by Lade *et al.* (1998). These were determined in order to indicate the relative densities of the silty sand specimens prepared for this study. Fig. 5 shows the influence of the fines content on the maximum and minimum void ratios. The variations of the maximum and minimum void ratios with fines content was discussed in detail and the guidelines indicated on this diagram are determined as indicated by Lade *et al.* (1998).

6. Volumetric compressibility

To obtain a comprehensive picture of the volumetric compressibility and its variation with fines content and relative density, a series of one-dimensional compression tests was performed on the silty sand mixtures. As for soft clays (Rutledge 1947), the volumetric compressibility of loose sand and sand with high compressibility tends to be controlled by the major principal stress (Lee and

Seed 1967). In a one-dimensional compression test, the vertical pressure is the major principal stress ($\sigma_{\max} = \sigma_{\text{vertical}}$), while the effective cell pressure in an isotropic compression test represents the major principal stress ($\sigma_{\max} = \sigma_{\text{cell}}$). The compressibilities of the silty sand mixtures determined from one-dimensional compression tests are therefore taken to represent the volumetric compressibilities from isotropic compression tests for the same values of the major principal stresses.

6.1 One-dimensional compression tests

For each of the silty sand mixtures described above, specimens were prepared in a steel consolidation ring with diameter of 10.16 cm (4.0 in.) and height of 2.54 cm (1.0 in.). Three specimens for each mixture were deposited inside the ring with relative densities of approximately 10, 50, and 85%. This was achieved by depositing a pre-weighed amount of silty sand through a funnel whose spout initially was placed on the bottom filter stone supporting the steel ring. The funnel was then slowly lifted up and moved around inside the steel ring to let the sand trickle out with negligible fall height. This method of sand deposition produces a relatively loose deposit. Specimens with higher relative densities were achieved by gently tapping the steel ring until the pre-weighed amount of soil fitted inside the ring with a level surface.

After carefully placing the top filter stone on the level silty sand surface, the specimen was loaded in increments from 0 to 200 kPa. Readings of vertical deformation were taken 2 minutes after each load increment in order to get consistent measurements with minimal influence of any time effects exhibited by the silty sand. The relation between vertical strain and the vertical pressure can be fitted with good accuracy by a power function expressed as (Schmidt 1967)

$$\varepsilon = a \cdot \left(\frac{\sigma}{p_a} \right)^b \quad (1)$$

in which p_a is atmospheric pressure expressed in the same units as the vertical stress, σ , and a and b are best-fitting parameters determined from the one-dimensional compression curve, as shown in

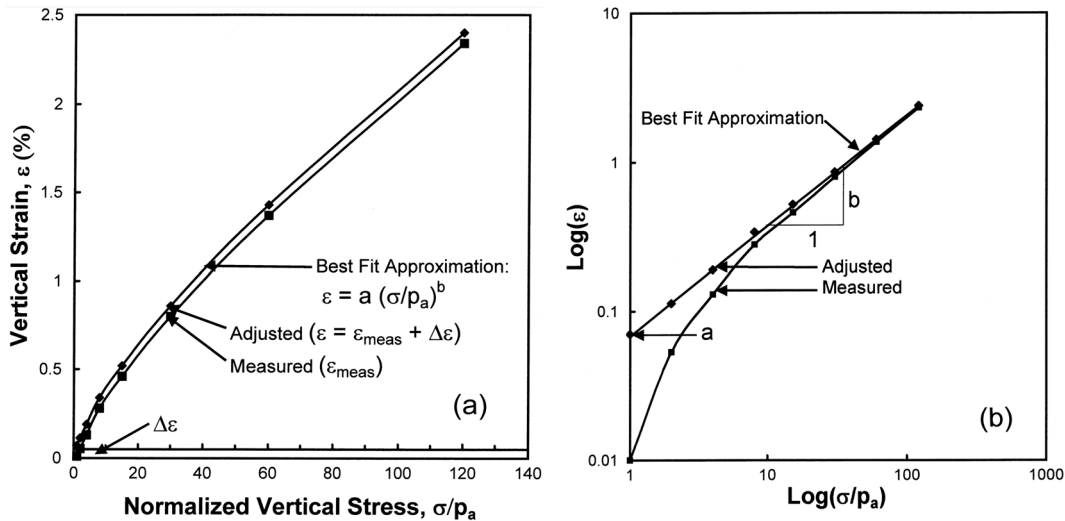


Fig. 6. Measured and adjusted one-dimensional compression curves shown on (a) arithmetic, and (b) log-log scales with best fitting lines for description by power function.

Fig. 6. The diagram in Fig. 6(a) shows a schematic diagram of the results of a typical one-dimensional compression curve.

To obtain the compressibility at a given pressure, the measured curve is first fitted with the expression given in Eq. (1). This is done by plotting the compression curve on log-log scales and fitting the best straight line, as shown in Fig. 6(b). Experience shows that the first pressure increment [from 0 to 10 kPa] produces a deformation increment slightly smaller than expected, i.e. the specimen appears to be stiffer for this first increment. Therefore, to achieve the best possible fit between experimental data and the power function in Eq. (1), a constant increment in strain, $\Delta\varepsilon$, is added to all the measured strains, as indicated in Fig. 6(a). The magnitude of this strain increment is determined with the goal of achieving the overall best fit between experimental data and Eq. (1). The addition of this strain increment has the effect of straightening the initially curved relationship, as shown in Fig. 6(b). The slope of the straight line is b and the intercept with $(\sigma/p_a) = 1$ is a .

The one-dimensional compression tests on the silty sand were performed in the range of pressures from 0 to 200 kPa with the first measurement recorded at 10 kPa. After fitting the experimental data as explained above, the volumetric compressibility was determined at 25 kPa (which is the isotropic consolidation pressure employed in the undrained triaxial compression tests) from Eq. (1) as follows

$$m_v = \frac{d\varepsilon}{d\sigma} = a \cdot b \cdot \left(\frac{\sigma}{p_a}\right)^{b-1} \quad (2)$$

in which $\sigma = 25$ kPa is substituted together with the values of a and b determined from each compression curve. Note that the translation of the compression curve along the ε -axis resulting from adding $\Delta\varepsilon$ to each strain measurement does not change the compressibility values obtained

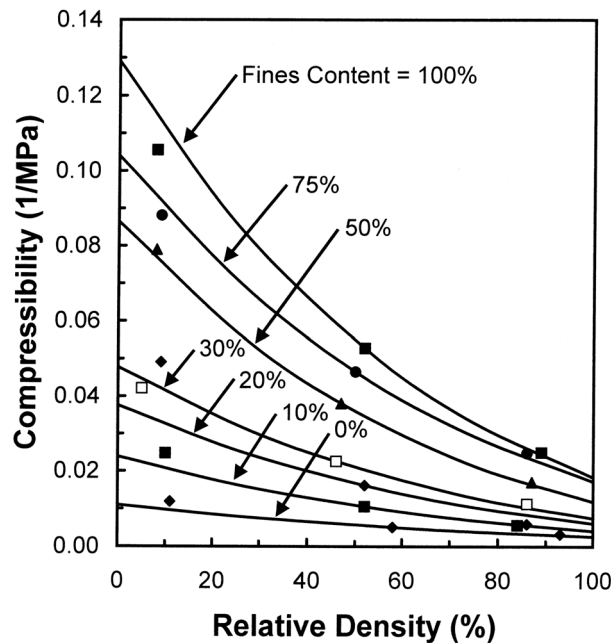


Fig. 7. Variation of compressibility of fine Ottawa sand and Loch Raven fines with fines content and relative density. Best fitting curves indicate systematic variation of compressibility.

from Eq. (2) in the range from 10 to 200 kPa.

Fig. 7 shows the variation of the individually determined compressibilities at 25 kPa for the seven different fines contents and three relative densities. The best fitting curves for all mixtures and relative densities are determined such that they form a consistent pattern, as seen in Fig. 7. This was done to overcome the scatter that invariably occurs in experimental results. This pattern of compressibilities will be related to the conditions for static liquefaction determined from the undrained triaxial compression tests presented below.

7. Undrained triaxial compression tests

7.1 Specimen Preparation and Saturation

The cap and base employed in the triaxial compression tests were supplied with lubricated ends consisting of two thin latex rubber sheets, each 0.015 mm (0.006 in.) thick, with a thin layer of silicone grease between. This lubrication system was very effective and caused the specimens to compress as right cylinders. To prevent the specimen from sliding out, the porous bronze drains located centrally in the cap and base, protruded slightly into the specimen. Cylindrical specimens with height = diameter = 97 mm (3.8 in.) were prepared by deposition of a pre-weighed amount of dry sand through a funnel with zero drop height into a rubber membrane held by a mold. The desired density was achieved by gently tapping the mold as necessary. Saturation was achieved by flushing the specimen with gaseous CO₂ for 30 min., after which de-aired water was allowed to percolate up through the sand, dissolving any CO₂ remaining in the specimen. A back pressure of 100 kPa was employed to help maintain full saturation during the undrained tests. B-value tests were performed to check the specimen saturation, and all specimens had B-values indicating full saturation, except those consisting of pure silt. It was more difficult to saturate the specimens with high silt contents, and those consisting of 100% silt were not fully saturated. While the specimens consisting of pure silt were tested, their results were used only to point to the likely relative densities at which liquefaction would occur. All undrained triaxial compression tests were performed with an initial consolidation pressure of 25 kPa and sheared at a strain rate of 0.1%/min. A 500 N load cell was employed to measure the axial deviator load with good accuracy.

7.2 Experimental program

Twenty eight undrained triaxial compression tests were performed to determine the void ratio for each sand mixture that would separate the condition of static liquefaction from stable behavior at the constant consolidation pressure of 25 kPa. Thus, for each sand mixture with a given fines content, an undrained test was first performed on a specimen with an arbitrary void ratio followed by additional tests with void ratios adjusted to capture the transition from static liquefaction to stable behavior. This trial-and-error approach resulted in the following number of tests at the respective fines contents: 1 test at 0% fines, 4 at 10%, 7 at 20%, 6 at 30%, 2 at 50%, 3 at 75%, and 5 tests at 100% fines for a total of 28 undrained triaxial compression tests. The results of the tests on specimens of pure silt will be used only to indicate the likely void ratio at which liquefaction would occur, because they were not fully saturated.

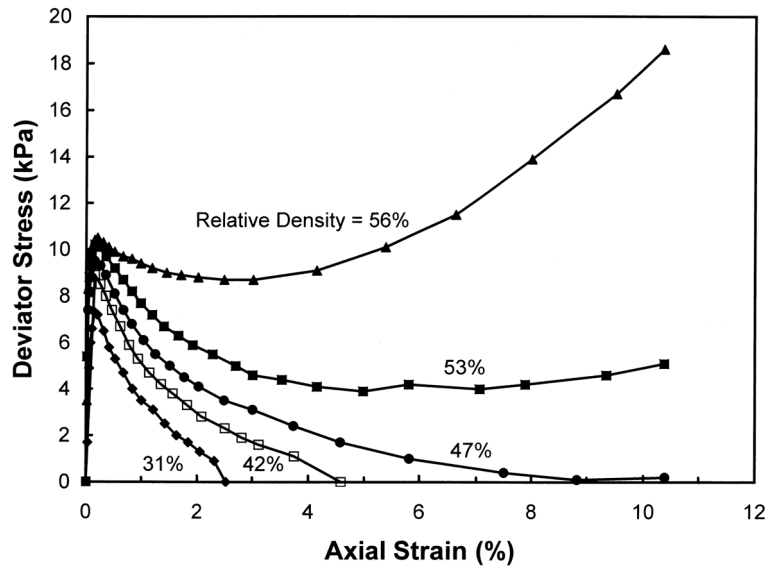


Fig. 8. Stress-strain curves for undrained triaxial tests on specimens of fine Ottawa sand and Loch Raven fines for a fines content = 20% and various relative densities performed to determine transition between stable behavior and static liquefaction.

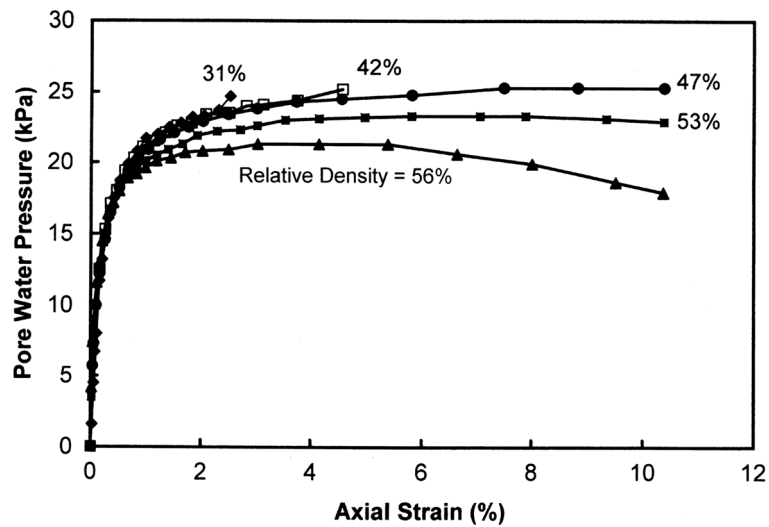


Fig. 9. Pore water pressure curves for undrained triaxial tests on specimens of fine Ottawa sand and Loch Raven fines for a fines content = 20% and various relative densities performed to determine transition between stable behavior and static liquefaction.

7.3 Results of undrained triaxial compression tests

The stress-strain and pore water pressure variations were plotted with axial strain and the effective stress paths were plotted in the Cambridge p' - q diagram for each silty sand mixture. As an example, the results for the mixture of 20% silt and 80% fine sand are shown in Figs. 8, 9, and 10. The

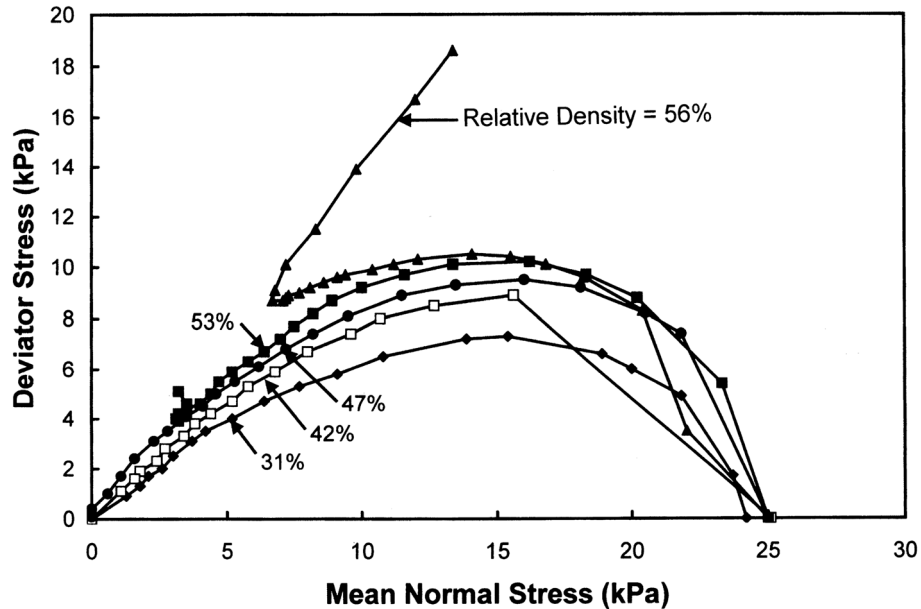


Fig. 10. Effective stress paths for undrained triaxial tests on specimens for a fines content = 20% and various relative densities performed to determine transition between stable behavior and static liquefaction.

results of 5 of 7 tests are shown with the two remaining tests being redundant and therefore not shown. The stress-strain relations in Fig. 8 clearly show the transition from liquefaction to stable behavior with increasing relative density. The pore pressure developments, shown in Fig. 9, are very similar and show very little influence over a range of relative densities of the silty sand, as for the 'reverse' behavior explained above. Fig. 10 shows the effective stress paths followed for each experiment in the 20-80 series of tests. The experiments were all terminated at 10% axial strain, because they had each revealed their individual type of behavior, liquefaction or stable behavior, within this range of axial strains. Thus, the undrained behavior for the stable specimens were not pursued beyond the 10% axial strain, because there was no further information to be obtained at higher strains for the present investigation. Besides, a 500 N load cell was employed to measure the axial deviator load with good accuracy, and this load cell did not permit continuation to much higher loads.

7.4 Interpretation of results

Judgment of the occurrence of stable behavior versus liquefaction is best performed from the stress-strain behavior shown in Fig. 8. As the relative density increases, the silty sand moves away from liquefaction and exhibits stable behavior. Three tests with $D_r = 31, 42,$ and 47% clearly show liquefaction, while two experiments on specimens with relative densities of 53% and 56% show stable behavior. Thus, the pivot position between stable behavior and liquefaction occurs near a relative density of 50% . Similar interpretations were made for the experimental results from the other silty sand mixtures, and the results are shown superimposed on the void ratio-fines content diagram in Fig. 11 and on the compressibility diagram in Fig. 12. Because the specimens consisting of 100% silt were not fully saturated, their results are only used to indicate where liquefaction may

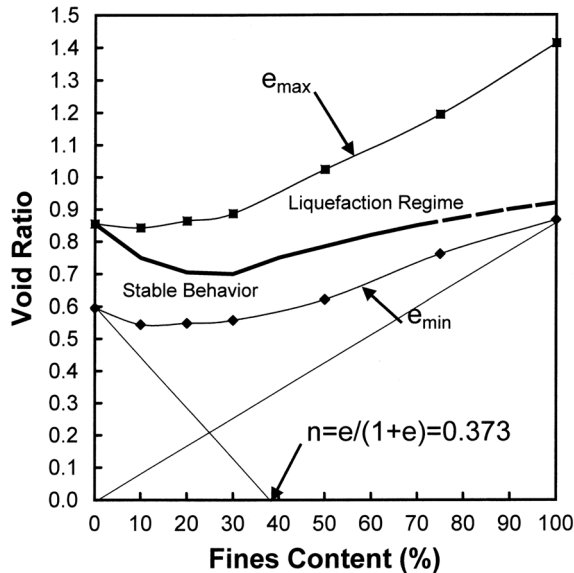


Fig. 11. Void ratio-percent fines diagram with indication of void ratios of specimens of fine Ottawa sand and Loch Raven fines in undrained triaxial tests at transition between stable behavior and static liquefaction.

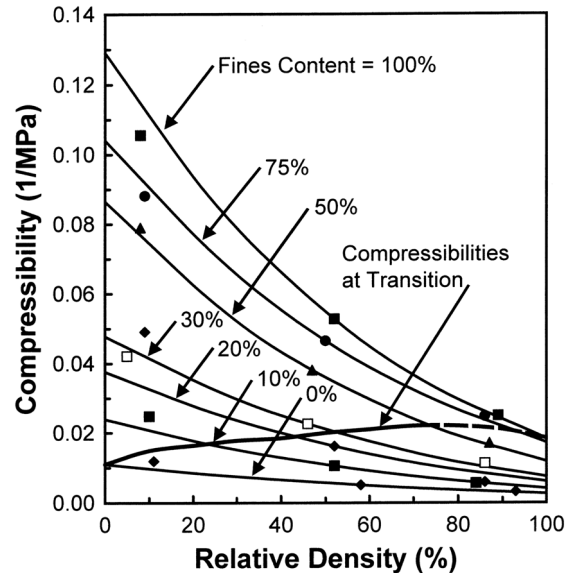


Fig. 12. Compressibility-relative density diagram with indication of compressibilities of specimens of fine Ottawa sand and Loch Raven fines in undrained triaxial tests at transition between stable behavior and static liquefaction.

occur, and the trend-lines indicated in Figs. 11 and 12 are therefore indicated as dotted lines in the range of high silt content. It is clear that the fines content plays an important role in the liquefaction potential of the silty sand. The greater the fines content, the higher is the relative density required for the silty sand to remain stable. It is also apparent that the volumetric compressibility plays an important role in this behavior. Fig. 12 shows that the greater volumetric compressibilities are associated with the higher liquefaction potential, because they facilitate development of higher pore pressures at small strains.

8. Compressibility as a measure of liquefaction potential

Thus, both the fines content and the relative density (or the void ratio) play important roles in liquefaction of silty sands. Fig. 13 shows the combined influence of these factors on a three-dimensional diagram in which the development of stable behavior and liquefaction are shown as dependent on volume compressibility, which in turn is dependent on fines content and void ratio. It appears that compressibilities in the range from 0.012 to 0.022 (1/MPa) and higher may lead to liquefaction under undrained conditions in the silty sand employed in this study. Limiting volumetric compressibilities for the Nevada sand with different fines contents tested by Yamamuro and Lade (1997, 1998) and Lade and Yamamuro (1997) were in the approximate range from 0.014 to 0.022 (1/MPa), i.e., very similar to those determined in the present investigation.

The void ratio, and therefore the steady-state diagram, has been shown to be ineffective in capturing the liquefaction behavior of loose silty sands (Yamamuro and Lade 1998). The behavior

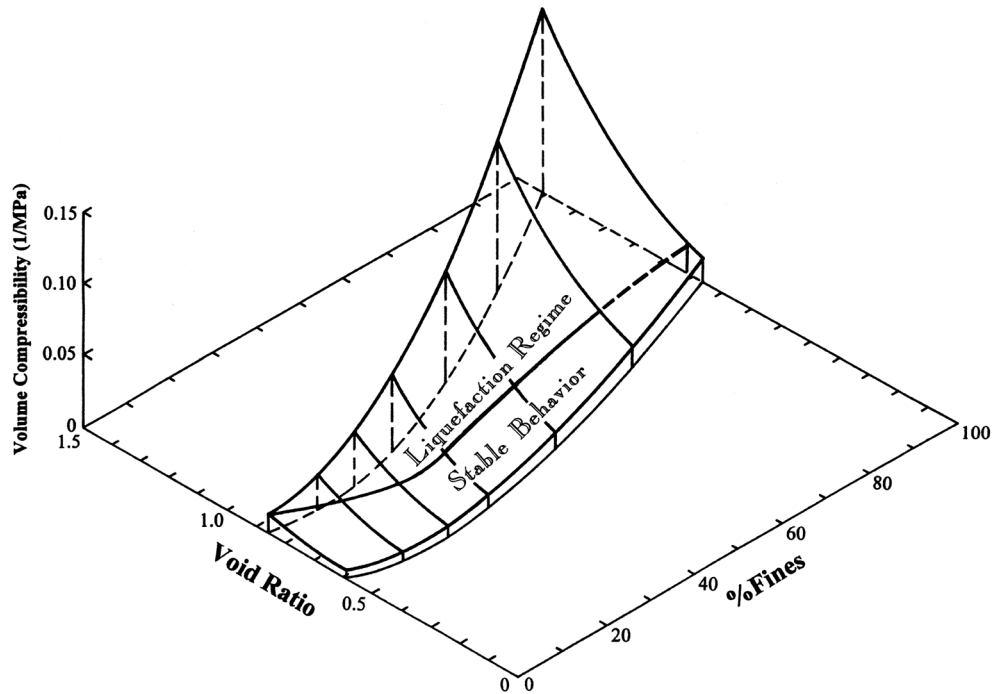


Fig. 13. Three-dimensional diagram showing static liquefaction related to volumetric compressibility, which in turn is influenced by fines content and void ratio for specimens of fine Ottawa sand and Loch Raven fines.

observed for loose silty sand at low confining pressures is ‘reverse’ of the normal behavior with regard to the effect of confining pressure, and this ‘reverse’ behavior causes liquefaction to occur at low pressures. The development of pore pressures under undrained conditions is directly related to the compressibility of the soil, and loose silty sands exhibit significant volumetric contraction at low pressures. Yamamuro and Lade (1998) proposed to use volumetric compressibility as an alternative indicator of liquefaction potential for silty sands.

Volumetric compressibility does not require determination of void ratio and fines content, and it can be measured in many different ways. For example, the last increment in isotropic compression before undrained shearing in a triaxial compression test may be used to obtain the volumetric compressibility. It may also be obtained from a standard oedometer test at the appropriate low stress magnitude, where the liquefaction potential is highest. Furthermore, it may be obtained from an in-situ test on the intact soil by inserting a screw-plate to relatively shallow depth and performing a plate load test to determine the vertical compressibility at the relevant field location. Such an in-situ test also captures the very important effect of the soil fabric or structure (Wood *et al.* 2008, Yamamuro *et al.* 2008) and avoids the difficult to impossible task of having to recover intact samples of the loose, silty sand for testing in the laboratory. Alternatively, a pressuremeter test may be employed to determine the compressibility in the horizontal direction. Whether the vertical or the horizontal compressibility is more relevant for indication of liquefaction potential remains to be seen. In addition, the actual boundary conditions in the field are important for determining the liquefaction potential in the field.

From knowledge of constitutive modeling of soils, it is logic that the volumetric compressibility is

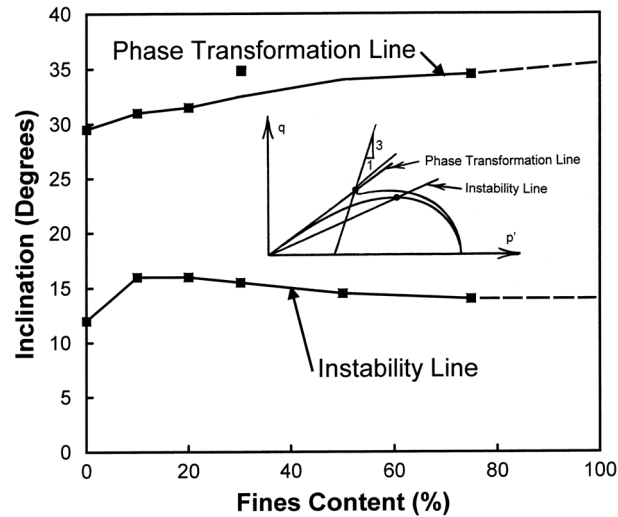


Fig. 14. Variation of inclinations of the phase transformation line and the instability line with fines content for fine Ottawa sand and Loch Raven fines.

one of the significant factors that control the development of pore pressures under undrained conditions. The fact that this property of a loose, silty sand deposit may be determined in-situ by a screw-plate test (vertical compressibility) (Schmertmann 1970, Janbu and Senneset 1973, Selvadurai and Nicholas 1979, Strout and Senneset 1998a, b) or by a pressuremeter test (horizontal compressibility) (Wroth 1975, Hughes *et al.* 1977, Fahey and Randolph 1984, Felio and Briaud 1986) at relatively shallow depths may make determination of liquefaction potential relatively easy. Besides, the fact that all significant factors that influence the volumetric compressibility are already present in the field deposit further increases the importance of such in-situ tests for indicating liquefaction potential.

9. Instability and phase transformation lines

The variations of the inclination of the instability and the phase transformation lines with fines content may also be obtained from the undrained experiments on the silty sand. Fig. 14 shows a diagram in which these quantities are shown varying with the fines content. The instability line is not much affected by the fines content and varies in the range between 12° and 16° . The inclination of the phase transformation line increases from 30° to about 35° as the fines content increases from 0% to 100%.

10. Conclusions

An experimental study has been performed to determine the effects of fines content in silty sand on the maximum and minimum void ratios, the compressibility and the potential for static liquefaction. The content of fines (particles smaller than 0.074 mm, i.e., passing the #200 U.S. sieve) in a fine sand was varied from 0% to 100% and experiments were conducted to determine the maximum and minimum void ratios, the volumetric compressibilities and the undrained behavior at a consolidation

pressure of 25 kPa. The volumetric compressibility at 25 kPa increases with increasing fines content and with decreasing relative density. The conditions that separate stable behavior from liquefaction were determined from 28 undrained triaxial compression tests performed on specimens with discrete fines contents and relative densities.

While the separation of stable behavior and liquefaction was determined as indicated, it was also observed that this separation was well-defined by a single property, namely the volumetric compressibility of the silty sand, which was nearly constant at this separation across the diagram of fines content and void ratio (or relative density). This observation has been made for two silty sands tested in undrained triaxial compression tests. The fact that compressibility relates to development of pore pressures under undrained conditions is logic on the basis of knowledge of constitutive modeling of soils, and it suggests that in-situ tests such as screw-plate tests and pressuremeter tests, from which the vertical and horizontal compressibilities can be determined, may be useful in directly indicating the liquefaction potential of soil deposits. This has the further advantage that it is independent of and therefore avoids having to determine void ratios, relative densities, and, most importantly, having to determine the soil fabric and reproducing this fabric in the laboratory.

References

- Fahey, M. and Randolph, M.F. (1984), "Effect of disturbance on parameters derived from self-boring pressuremeter in sand", *Geotechnique*, **34**(1), 81-97.
- Felio, G.Y. and Briaud, J.L. (1986), "Conventional parameters from pressuremeter test data: Review of existing methods", *The Pressuremeter and Its Applications*, Second International Symposium, ASTM STP 950, American Society for Testing and Materials, Philadelphia, 265-282.
- Hughes, J.M.O., Wroth, C.P. and Windle, D. (1977), "Pressuremeter Tests in Sand", *Geotechnique*, **27**(4), 455-477.
- Janbu, N. and Senneset, K. (1973), "Field compressometer – principles and applications", *Proceedings of the Eighth international Conference on Soil Mechanics and Foundation Engineering*, Moscow, **1.1**, 191-198.
- Lade, P.V. (1992), "Static instability and liquefaction of loose fine sandy slopes", *J. Geotech. Eng., ASCE*, **118**(1), 51-71.
- Lade, P.V. (1993), "Initiation of static instability in the submarine Nerlerk berm", *Can. Geotech. J.*, **30**(5), 895-904.
- Lade, P.V. (1994a), "Creep effects on static and cyclic instability of granular soils", *J. Geotech. Eng., ASCE*, **120**(2), 404-419.
- Lade, P.V. (1994b), "Instability and liquefaction of granular materials", *Comput. Geotech.*, **16**, 123-151.
- Lade, P.V., Liggio, C.D. Jr., and Yamamuro, J.A. (1998), "Effects of non-plastic fines on minimum and maximum void ratios of sand", *Geotech. Test. J.*, ASTM, GTJODJ, **21**(4), 336-347.
- Lade, P.V., Nelson, R.B. and Ito, Y.M. (1987), "Nonassociated flow and stability of granular materials", *J. Eng. Mech., ASCE*, **113**(9), 1302-1328.
- Lade, P.V., Nelson, R.B. and Ito, Y.M. (1988), "Instability of granular materials with nonassociated flow", *J. Eng. Mech., ASCE*, **114**(12), 2173-2191.
- Lade, P.V. and Pradel, D. (1990), "Instability and plastic flow of soils, I: Experimental observations", *J. Eng. Mech., ASCE*, **116**(11), 2532-2550.
- Lade, P.V. and Yamamuro, J.A. (1997), "Effects of non-plastic fines on static liquefaction of sands", *Can. Geotech. J.*, **34**(6), 918-928.
- Lee, K.L. and Seed, H.B. (1967), "Drained strength characteristics of sands", *J. Soil Mech. Found. Division, ASCE*, **93**(SM6), 117-141.
- Rutledge, P. (1947), "Cooperative triaxial shear research program of the corps of engineers, triaxial shear research distribution studies on soils", Waterways Experiment Station, Vicksburg, Mississippi, 1-178.

- Schmidt, B. (1967), "Uniaxial primary compression of sands", Bulletin No. 23, The Danish geotechnical Institute, 13-26.
- Schmertmann, J.H. (1970), "Suggested method for screw-plate load test", *Special Procedures for Testing Soils and Rock for Engineering Purposes*, ASTM STP 479, 81-85.
- Selvadurai, A.P.S. and Nicholas, T.J. (1979), "A theoretical assessment of the screw plate test", *Proceedings of the 3rd International Conference on Numerical methods in Geomechanics*, Aachen, West Germany, 1245-1252.
- Strout, J.M. and Senneset, K. (1998a), "International development of the field compressometer", *Proceedings of the First International Conference on Site Characterization*, Atlanta, Georgia, 2, 857-862.
- Strout, J.M. and Senneset, K. (1998b), "The field compressometer test in Norway", *Proceedings of the First International Conference on Site Characterization*, Atlanta, Georgia, 2, 863-868.
- Wood, F.M., Yamamuro, J.A. and Lade, P.V. (2008), "Effect of depositional method on the undrained response of silty sand", *Can. Geotech. J.* (accepted).
- Wroth, C.P. (1975), "In Situ measurement and initial stresses and deformation characteristics", *Proceedings of the Conference on In Situ Measurement and Soil Properties*, ASCE, Vol. II, North Carolina, 181-230.
- Yamamuro, J.A. and Lade, P.V. (1997), "Static liquefaction of very loose sands", *Can. Geotech. J.*, 34(6), 905-917.
- Yamamuro, J.A. and Lade, P.V. (1998), "Steady state concepts and static liquefaction of silty sands", *J. Geotech. Geoenviron. Eng., ASCE*, 124(9), 868-877.
- Yamamuro, J.A. and Lade, P.V. (1999), "Experiments and modelling of silty sands susceptible to static liquefaction", *Mech. Cohesive-Frictional Mater.*, Wiley, 4(6), 545-564.
- Yamamuro, J.A., Wood, F.M. and Lade, P.V. "Effect of depositional method on the microstructure of silty sand", *Can. Geotech. J.* (accepted).
- Zlatovic, S. and Ishihara, K. (1997), "Normalized behavior of very loose non-plastic soils: Effects of fabric", *Soils Found.*, 37(4), 47-56.